Sec16A defines the site for vesicle budding from the endoplasmic reticulum on exit from mitosis

Helen Hughes and David J. Stephens*

Cell Biology Laboratories, School of Biochemistry, Medical Sciences Building, University of Bristol, University Walk, Bristol, BS8 1TD, UK

*Author for correspondence (david.stephens@bristol.ac.uk)

Accepted 26 August 2010
Journal of Cell Science 123, 4032-4038

doi:10.1242/jcs.076000

Summary

Mitotic inhibition of COPII-dependent export of proteins from the endoplasmic reticulum results in disassembly of the Golgi complex. This ensures ordered inheritance of organelles by the two daughter cells. Reassembly of the Golgi is intimately linked to the re-initiation of ER export on exit from mitosis. Here, we show that unlike all other COPII components, which are cytosolic during metaphase, Sec16A remains associated with ER exit sites throughout mitosis, and thereby could provide a template for the rapid assembly of functional export domains in anaphase. Full assembly of COPII at exit sites precedes reassembly of the Golgi in telophase.

Key words: COPII, Golgi, Mitosis

Introduction

The inheritance of organelles during mitosis is essential to ensure the proper organisation and function of successive cell generations. The Golgi is a single copy organelle and as such is dispersed throughout the cytoplasm before inheritance to ensure distribution between both daughter cells (Wei and Seemann, 2009). This is achieved through two means, the dispersion of structural components of the Golgi complex to a peripheral distribution (Lucocq and Warren, 1987; Shima et al., 1997; Seemann et al., 2002) and absorption of other components with the ER [such as Golgi glycosylation enzymes (Storrie et al., 1998; Zaal et al., 1999)]. Many resident glycosylation enzymes of the Golgi complex cycle slowly through the ER during interphase (Storrie et al., 1998). Export of secretory cargo from the ER is inhibited during mitosis (Prescott et al., 2001) and therefore these enzymes accumulate in the ER and are inherited via equal partitioning of this compartment. In other cases, separation of the ER and Golgi through mitosis is essential to ensure segregation of key signalling components that would become activated if localised together (Bartz et al., 2008).

The integrity of the Golgi complex depends on ongoing transport from the ER (Ward et al., 2001). ER export (for a review, see Hughes and Stephens, 2008) is mediated by the COPII coat, which assembles at sites on the ER membrane known as transitional ER (tER). COPII assembly is directed by the Sar1 GTPase, which, following activation by Sec12, directs sequential recruitment of Sec23-Sec24 and Sec13-Sec31. Together, these components form a vesicle coat that selects cargo for export, deforms the membrane, and ultimately generates coated transport vesicles following budding. An additional component, Sec16, potentiates budding (Supek et al., 2002) and appears to mark the transitional ER membrane and define the site of COPII vesicle budding (Connerly et al., 2005; Ivan et al., 2008; Hughes et al., 2009). Inhibition of vesicle budding from the ER during prometaphase (Farmaki et al., 1999) correlates with the loss of COPII proteins (Sec23-Sec24 and Sec13-31) from the ERES membrane (Farmaki et al., 1999; Hammond and Glick, 2000; Prescott et al., 2001; Stephens, 2003; Altan-Bonnet et al., 2006). This pre-budding arrest of COPII-dependent trafficking results in Golgi disassembly and can be induced experimentally in interphase through inhibition of COPII function [for example, by blocking the GTPase cycle of Sar1 (Kuge et al., 1994)]. In telophase, the Golgi reassembles through re-initiation of ER export activity. This results in re-formation of the Golgi stack and repopulation with Golgi-resident proteins (Souter et al., 1993; Altan-Bonnet et al., 2006).

Because ER export activity directs Golgi reassembly, it is important to understand the spatial coordination of the onset of ER export on exit from mitosis. In *Trypanosoma brucei*, centrin2 localises to a bi-lobed structure, one lobe lying adjacent to the old Golgi with the other defining the localisation of the new Golgi during duplication (He et al., 2005). Although the Golgi in interphase mammalian cells lies adjacent to the centrosome, it is not obvious how a centrosomal protein could reorganise peripherally dispersed Golgi elements on exit from mitosis. We have previously shown that the principle human orthologue of Sec16, Sec16A (Watson et al., 2006), localises to the transitional ER membrane independently of other COPII proteins (Hughes et al., 2009). Sec16A interacts with COPII proteins [at least Sec23 (Bhattacharyya and Glick, 2007; Iinuma et al., 2007) and Sec13 (Hughes et al., 2009)] and could therefore act in directing the assembly of COPII on the transitional ER membrane before vesicle formation. In interphase, this probably serves to optimise COPII assembly at ERES. Computational modelling of COPII assembly has shown that such directed recruitment of Sar1, Sec23–Sec24 and Sec13–Sec31 (i.e. biased binding to a predefined site) more accurately describes the organisation of ERES seen in mammalian cells (Heinzer et al., 2008). Notably, this model does not include Sec16 itself, but intriguingly, the model initiates from a naked membrane with no prior membrane localisation of COPII proteins. This situation is analogous to that occurring when cells exit mitosis with COPII proteins Sar1, Sec23–Sec24, and Sec13–Sec31 localised to the cytosol.

Using quantitative 4D imaging of cells, we show that Sec16A remains associated with the ER membrane throughout mitosis and defines the localisation for the re-initiation of COPII-dependent budding on exit from mitosis.

Results and Discussion

We generated a stable HeLa cell line expressing Venus–Sec16AΔN, a construct that lacks the N-terminal 1008 amino acids of Sec16A, yet behaves in an indistinguishable manner to transiently transfected fluorescent protein (FP)-tagged Sec16A or to endogenous Sec16A (supplementary material Fig. S1). We were unable to generate stable cell lines expressing FP-Sec16A by plasmid transfection. Lentiviral transduction of FP–Sec16A was precluded by persistent recombination of the parent vector during cloning. Importantly, Venus–Sec16AΔN includes both the central conserved domain and upstream sequences shown to be necessary for membrane association and targeting to ERES (Ivan et al., 2008; Hughes et al., 2009). Specifically, it colocalises exactly with endogenous Sec16A and localises adjacent to Sec24C and Sec31A labelling, as is seen for endogenous Sec16A (Hughes et al., 2009); its expression does not alter the expression of endogenous Sec16A, and it rescues the phenotypes of decreased ERES number and Golgi fragmentation caused by suppression of endogenous Sec16A (supplementary material Fig. S1). We visualised Venus–Sec16AΔN-expressing HeLa cells throughout mitosis in 4D using spinning disk confocal microscopy. This approach provides excellent 3D spatial information over time without significant photobleaching. Fig. 1A (enlarged in Fig. 1B) shows that Venus–Sec16AΔN remained associated with defined puncta throughout mitosis [fluorescence and differential interference contrast (DIC) images, see also supplementary material Movie 1]. During fluorescence recovery after photobleaching (FRAP) experiments, Venus–Sec16AΔN showed similar dynamics to full-length GFP–Sec16A (Hughes et al., 2009) with $t_{1/2}$=~8 seconds (Fig. 1C). Images and further quantification of these experiments is shown in supplementary material Fig. S2. The rate of cycling was not significantly affected by the transition from interphase to mitosis. This suggests that membrane association of Sec16 is not subject to mitotic regulation. However, it does not preclude mitotic inhibition of interactions of Sec16 with downstream COPII components (Altan-Bonnet et al., 2006). Although the mechanisms underlying this inhibition remain unknown, these data also reinforce previous data showing that Sar1, Sec23–Sec24, Sec13–Sec31 all lie downstream of Sec16 (Ivan et al., 2008; Hughes et al., 2009).

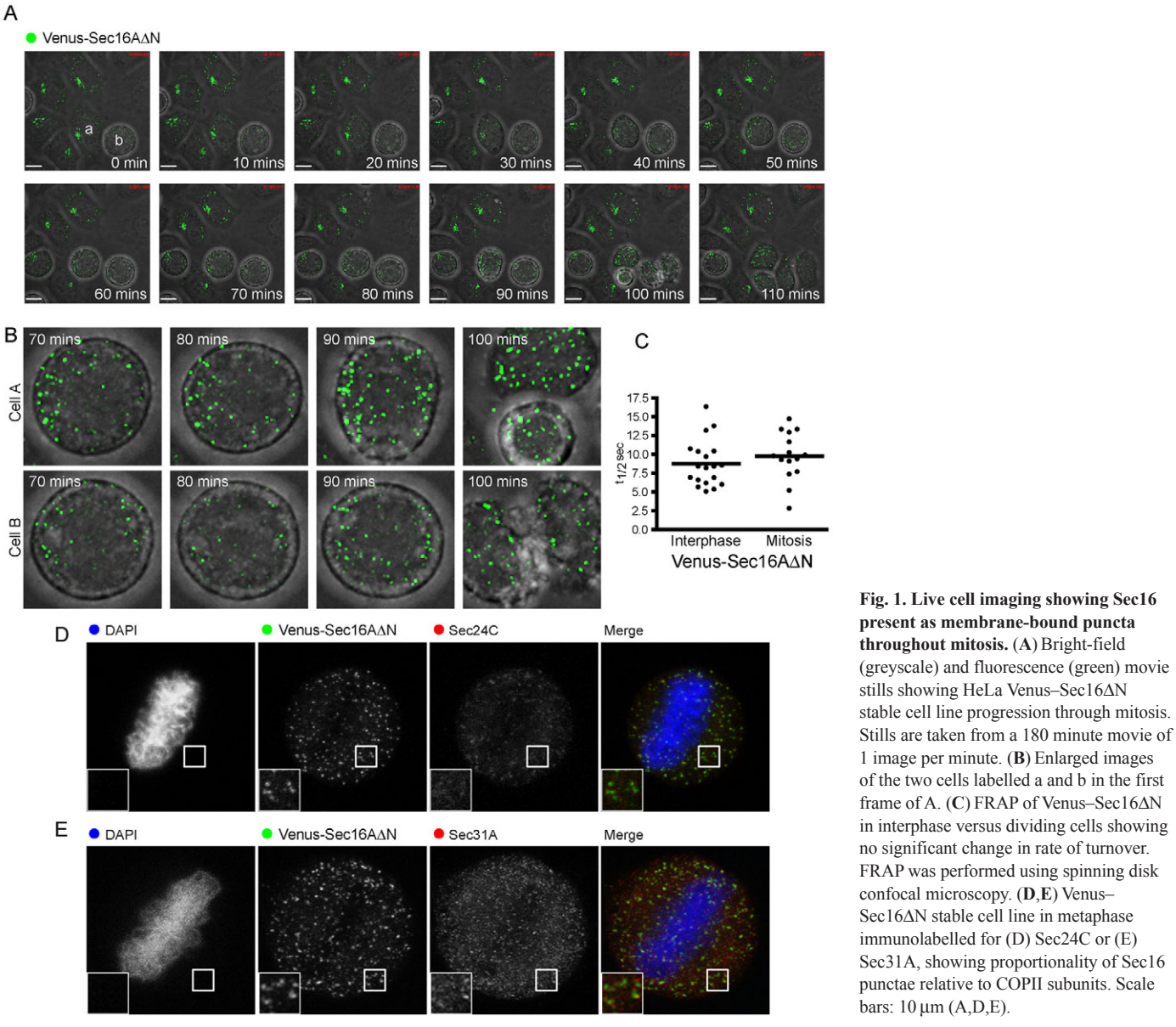

Fig. 1. Live cell imaging showing Sec16 present as membrane-bound puncta throughout mitosis. (**A**) Bright-field (greyscale) and fluorescence (green) movie stills showing HeLa Venus–Sec16ΔN stable cell line progression through mitosis. Stills are taken from a 180 minute movie of 1 image per minute. (**B**) Enlarged images of the two cells labelled a and b in the first frame of A. (**C**) FRAP of Venus–Sec16ΔN in interphase versus dividing cells showing no significant change in rate of turnover. FRAP was performed using spinning disk confocal microscopy. (**D**,**E**) Venus–Sec16ΔN stable cell line in metaphase immunolabelled for (D) Sec24C or (E) Sec31A, showing proportionality of Sec16 punctae relative to COPII subunits. Scale bars: 10 μm (A,D,E).

In fixed cells expressing Venus–Sec16AΔN, other COPII proteins, Sec24C (Fig. 1D) and Sec31A (Fig. 1E) were largely redistributed to the cytosol, as has been described previously (Farmaki et al., 1999; Stephens, 2003). Several Sec16A-positive puncta were apparent that do not show adjacent labelling of Sec24C (Fig. 1D) or Sec31A (Fig. 1E). We sought to validate these findings by accumulating cells in mitosis using a series of small molecule inhibitors. Monastrol is a cell-permeable inhibitor of the mitotic kinesin Eg5 (Mayer et al., 1999); its mode of action results in the accumulation of cells with monopolar spindles in mitosis. BI2536 is an inhibitor of polo-like kinase 1, which also arrests cells in mitosis (Steegmaier et al., 2007). UA62784 inhibits the function of CENP-E, thereby preventing proper chromosome congression in metaphase (Henderson et al., 2009). Application of each of these three inhibitors led to accumulation of cells in mitosis that showed clear localisation of Venus–Sec16AΔN to puncta, but loss of Sec24C and Sec31A to a cytosolic distribution (supplementary material Fig. S3). Labelling for other markers [giantin and galactosyltransferase (GalT)] confirmed Golgi dispersal. These data confirm our findings from unperturbed cells during mitosis.

Similarly to Venus–Sec16AΔN, endogenous Sec16A localises to defined puncta throughout mitosis (Fig. 2). This is in stark contrast to previous findings using other COPII proteins, which redistribute to the cytosol during metaphase (Farmaki et al., 1999; Stephens, 2003; Altan-Bonnet et al., 2006). Double labelling with antibodies specific for the Sec31A subunit of the COPII coat (Fig. 2) showed that, as has been previously described, Sec31A remained localised to puncta during interphase and prometaphase. At metaphase (when chromosome are tightly aligned on the metaphase plate) Sec31A was largely lost from discrete puncta (Fig. 2, see boxed enlargements); however, as we have described previously (Stephens, 2003), fixation of cells for immunolabelling enhances the appearance of punctate labelling. Notably these remaining puncta of Sec31A often do not align adjacent to Sec16A and therefore we would not characterise these as functional ERES (see Hughes et al., 2009).

To validate our findings in living cells without potential artefacts from cell fixation, we imaged cells stably expressing both Venus–Sec16AΔN and mRuby–Sec23A. A lentivirus expressing mRuby–Sec23A was constructed by switching the fluorescent protein tag from EYFP–Sec23A, which we have previously successfully used for similar experiments (Stephens, 2003). Control experiments showed that mRuby–Sec23A localised as expected to puncta perfectly aligned with Sec24C and Sec31A but offset from endogenous Sec16A (data not shown). Furthermore, in cells either singly expressing mRuby–Sec23A or doubly transfected cells coexpressing both Venus–Sec16AΔN and mRuby–Sec23A the structure of the Golgi (giantin labelling) and the localisation of GalT (as a marker of the efficiency of ER-to-Golgi transport) in cells were indistinguishable from that of non-transfected cells (data not shown). The rate of mitotic progression was also unaffected by stable transfection of either mRuby–Sec23A alone or of both Venus–Sec16AΔN and mRuby–Sec23A (data not shown). We observed that although Venus–Sec16AΔN remained associated with tER membranes throughout mitosis (Fig. 3A), mRuby–Sec23A dissociated from ERES during metaphase (Fig. 3B and supplementary material Movie 2). Contrast enhancement showed some detectable punctate localisation of mRuby–Sec23A, which could not easily be distinguished from background (Fig. 3C, arrow). These objects did not lie adjacent to Venus–Sec16AΔN-labelled puncta and therefore would not be defined as bona fide ERES (Hughes et al., 2009). Furthermore, FRAP analysis showed that,

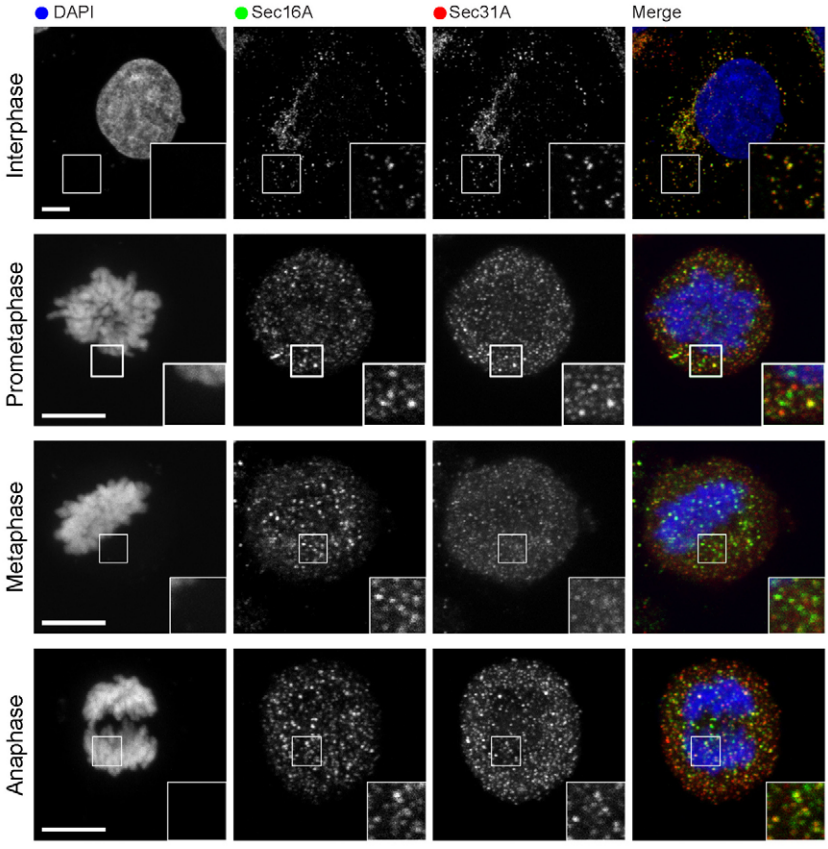

Fig. 2. Endogenous Sec16 and COPII subunit localisation during cell division. Fixed cells were labelled to detect endogenous Sec16A and the COPII subunit Sec31A at various stages of cell division. DAPI labelling of DNA was used to define the mitotic state of cells as indicated and 3D stacks of images were acquired to image the entire depth of the cells. Scale bars: 10 μm.

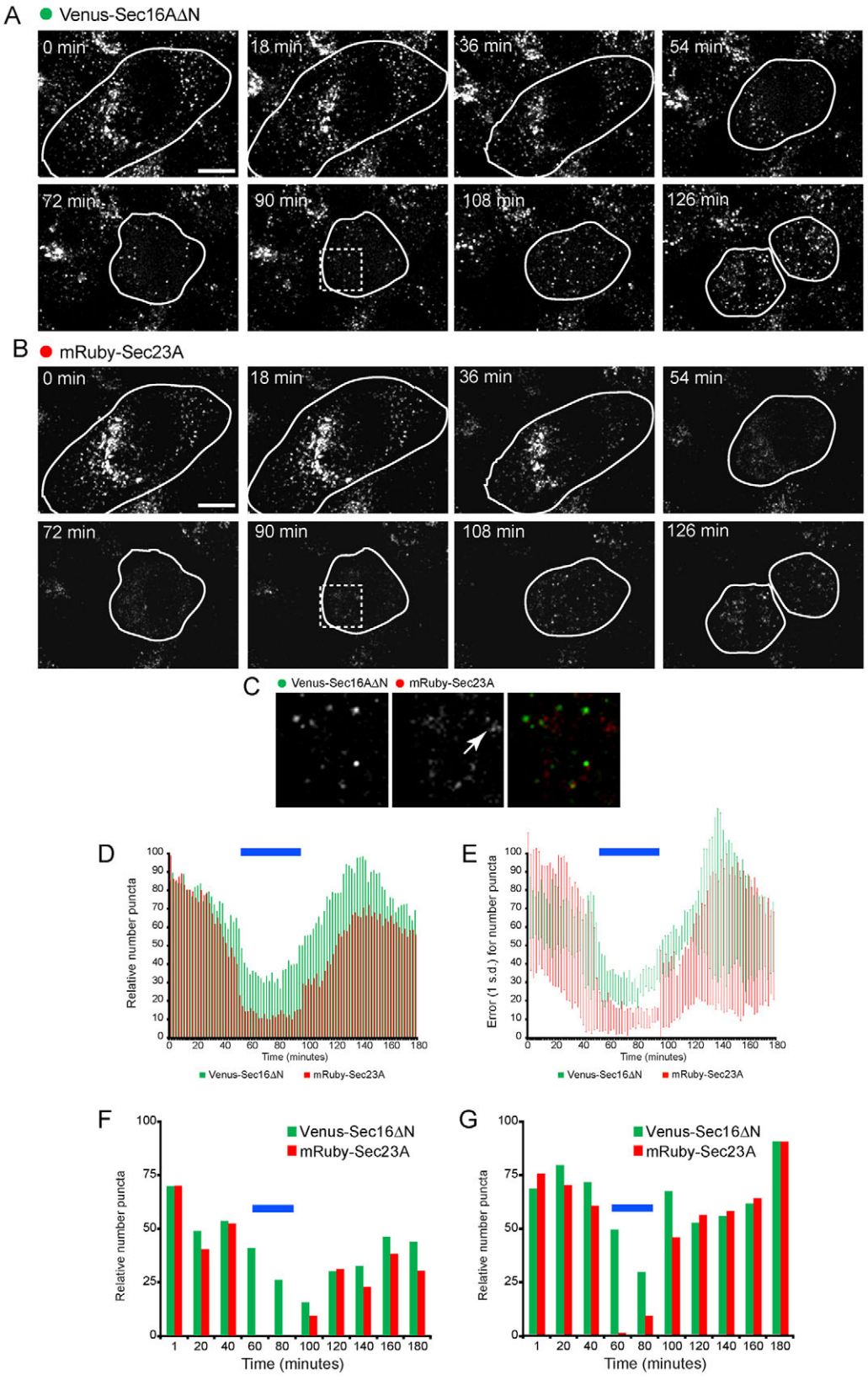

Fig. 3. Quantification of Venus–Sec16ΔN versus mRuby–Sec23A during mitosis. (**A**,**B**,**C**) Cells expressing both Venus–Sec16ΔN and mRuby–Sec23A imaged through cell division. 1 *z*-stack (22 slices with 1 µm spacing shown as a maximum intensity projection) was acquired every 2 minutes over a total of 180 minutes. Scale bars: 5 µm. Enlargements of the boxed regions from A and B are shown in C. (**D**) Automated quantification of the relative number of puncta present within cells expressing both Venus–Sec16AΔN (green) and mRuby–Sec23A (red) that were undergoing mitosis (quantification of five cells from three independent experiments). (**E**) Error bars for the data in D show 1 s.d., the blue bar indicates those time point for which there is a statistically detectable (*t*-test, $P<0.05$) difference between the two channels [Venus–Sec16AΔN (green) and mRuby–Sec23A (red)]. (**F**,**G**) Quantification of every tenth frame from two individual examples of cells going through mitosis. Blue bars highlight those time points where there are no detectable mRuby–Sec23A-labelled puncta despite the persistence of Venus–Sec16AΔN-labelled puncta.

unlike during interphase, these mRuby–Sec23A-positive structures in metaphase did not recover fluorescence after photobleaching (HH and DJS unpublished observations) indicating that they are not functionally the same as ERES. They might represent clusters of Sec13p-labelled membrane tubules as previously observed by immunoelectron microscopy (Farmaki et al., 1999). We speculate that the punctae are more likely to be vesicular-tubular remnants resulting from juxtanuclear ERES clustering and Golgi breakdown.

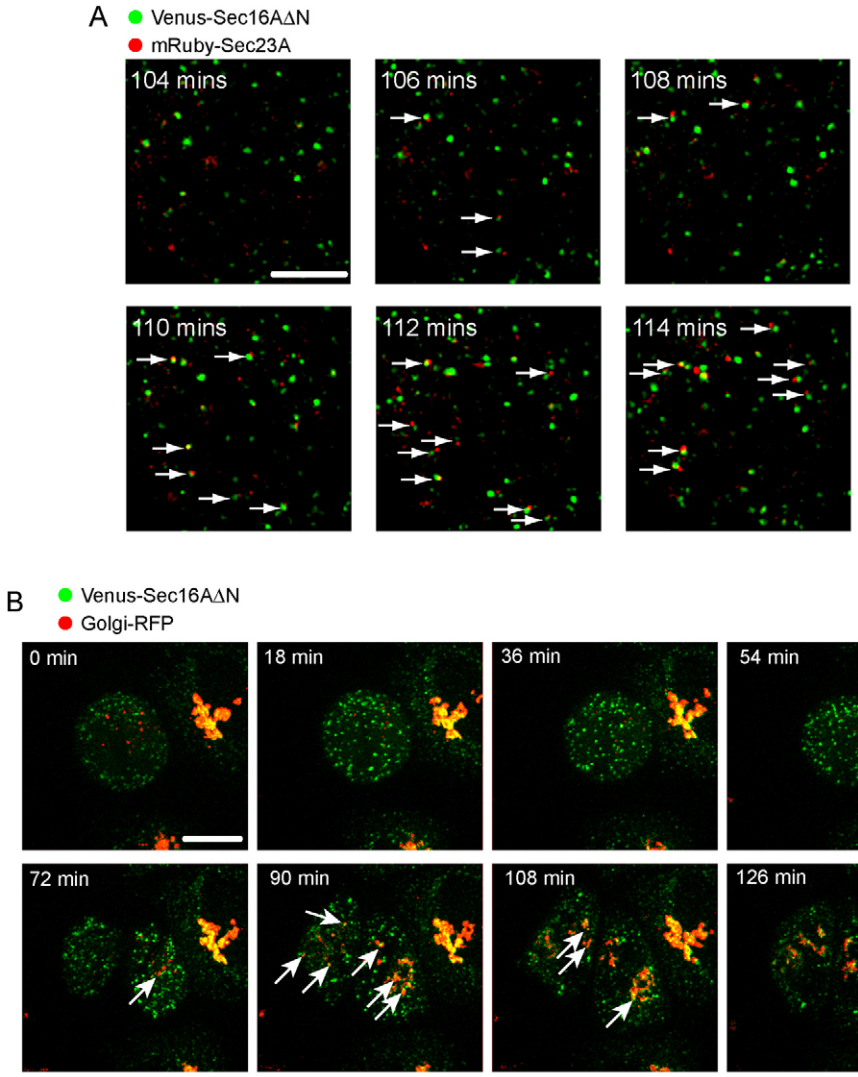

Fig. 4. (**A**) mRuby–Sec23A-positive ERES emerge from Venus–Sec16ΔN-positive tER sites on exit from metaphase (arrows). Images show enlargements of cells expressing both markers where 3D stacks (22 *z*-slices with 1 µm spacing shown as a maximum intensity projection) of cells exiting metaphase were acquired at 2 time points per minute. Arrows indicate Venus–Sec16ΔN-positive punctae from which mRuby–Sec23A punctae appear to emerge. (**B**) Imaging of Golgi–RFP (red) and Venus–Sec16ΔN (green) on exit from mitosis, shows that the Golgi (arrows) forms at a juxtanuclear region adjacent to clustered ERES. Images show maximum intensity projections of 21 *z*-slices acquired with 1 µm spacing. Scale bars: 5 µm (A) and 10 µm (B).

Automated quantification of multiple experiments (automatically detecting and counting all ERES in total of 15 dividing cells) confirmed these observations (Fig. 3D). The number of discrete objects labelled with Venus–Sec16AΔN decreased by around 70% as cells enter metaphase. The loss of mRuby–Sec23A from discrete puncta was more pronounced, with <10% detectable objects per cell remaining. Our quantification method was based purely on intensity and so will include any sufficiently bright object within the field of view including mitotic ERES remnants (Farmaki et al., 1999). This, along with the increase in ERES association of Sec23A in cells expressing Venus–Sec16AΔN means that these data overestimate the number of discrete mRuby–Sec23A-labelled objects. The standard deviations of five averaged time sequences (Fig. 3E) further validated these observations and revealed a clear statistically detectable difference in numbers of Venus–Sec16AΔN and mRuby–Sec23A puncta. Frame-by-frame quantification (Fig. 3F,G) showed that we frequently did not observe any visible Sec23A-labelled puncta in metaphase cells (as indicated by the blue bars on these graphs). By contrast, we have never observed cells during metaphase that do not contain obvious Venus–Sec16AΔN puncta. Automated quantification of the intensity of objects revealed that although they are smaller, the mean intensity of individual spots was unchanged through mitosis (not shown).

The number of Venus–Sec16AΔN puncta increased on exit from metaphase (around 100 minutes from the start of the time series) and preceded an increase in mRuby–Sec23A-labelled objects. This is consistent with the idea that Sec16A precedes Sec23A during COPII assembly. Indeed, on exit from mitosis, we observed that mRuby–Sec23A-labelled puncta emerged in close apposition to Venus–Sec16AΔN-labelled structures (Fig. 4A, arrows highlight close juxtaposition of Venus–Sec16AΔN and mRuby–Sec23A, see supplementary material Movie 2). This also preceded re-formation of the Golgi, which occurs in late telophase (Fig. 4B, arrows highlight reforming Golgi clusters, see supplementary material Movie 3). Golgi structures appeared to emerge in the vicinity of the centrosomes, consistent with a role for microtubules in directing the spatial organisation of the reforming of the Golgi ribbon (Ho et al., 1989; Corthesy-Theulaz et al., 1992) as well as increasing the efficiency of the ER export and ER-to-Golgi transport (Watson et al., 2005; Palmer et al., 2009).

Our data show that Sec16A marks the transitional ER throughout mitosis and is coincident with the reappearance of COPII puncta on exit from metaphase. These data are entirely consistent with our previous findings that siRNA-mediated depletion of Sec16A results in a decrease in the number of ERES within a cell (Watson et al., 2006). By directing ERES assembly, Sec16A ensures that

intracellular architecture of the cell is restored quickly and effectively on exit from mitosis. Two major outstanding mechanisms remain to be defined – how Sec16A itself is targeted to the ERES membrane and how Sec16A is uncoupled from other COPII proteins during mitosis.

Materials and Methods

Generation of cDNA constructs and generation of stable cell lines

cDNAs encoding both Venus fluorescent protein (Nagai et al., 2002) and Sec16ΔN were amplified by PCR and subcloned via pGEM-T vector. Venus was excised with *Bgl*II-*Sbf*I for insertion into a modified HIV-1-based self-inactivating pSEW sin lentiviral vector backbone lacking the WPRE region (kindly provided by Giles Cory, University of Exeter, Exeter, UK) via *Bam*HI-*Sbf*I. pHRSINcPPT-SEW-Venus was further digested via *Bam*HI-*Sbf*I for insertion of Sec16ΔN (excised from pGEM via *Bgl*II-*Sbf*I). Virus preparation was undertaken using HEK293T cells in a 10 cm culture dish at 80% confluence. 40 μg vector construct, alongside packaging vectors pMDG 2 (10 μg) and p8.91 (30 μg) were combined in 5 ml Optimem. A 1:1 solution of DNA:PEI (2 mM in Optimem) was incubated for 20 minutes before adding drop-wise to washed cells. The cells were incubated at 37°C, 5% CO_2 for 4 hours before replacing with complete DMEM. 48 hours after the transfection, viral particles were harvested and added to HeLa cells at 70% confluence. Cells were left to grow for 2 weeks post-confluence, Venus-expressing colonies were determined by light microscopy, picked and replated to produce a clonal Venus-Sec16ΔN stable cell line. The cDNA sequence encoding mRuby (Kredel et al., 2009) underwent codon usage adaptation before gene synthesis (MWG Eurofins) and cloning into pBluescript II SK(+). mRuby was excised with *Sal*I-*Eco*RI for insertion into pLVX-Puro (Clontech) to generate pLVX-Puro–mRuby. A cDNA encoding human Sec23A was amplified by PCR, gel purified and subcloned via pGEM-T vector (excised with *Apa*I-*Xba*I) and cloned into pLVX-Puro–mRuby. Lentivirus preparation followed the Clontech Lenti-X. mRuby–Sec23A-expressing cells were selected using puromycin.

Cell synchronisation

Cell synchronisation was achieved using a double thymidine block. Cells grown to 40% confluency were subjected to 2 mM thymidine for 16 hours. Cells were washed three times with PBS, and incubated for 8 hours in complete medium, before repeating the block and wash-out. Cells undergo mitosis 12 hours after second wash-out.

Mitotic inhibitors

Inhibitors were incubated in complete medium at the following concentrations; 100 μM Monastrol, 100 nM BI 2536, 500 nM UA 62784 for 6 hours after the second wash-out before PFA fixation.

Imaging of fixed cells

PFA-fixed immunolabelled cells were imaged using Leica TCS-SP4 AOBS scanning confocal microscope and processed using Photoshop 6.0 (Adobe, Uxbridge, UK) and montages generated using Adobe Illustrator (Adobe). To provide the highest degree of accuracy, Nyquist sampling theorem was applied to ascertain the correct voxel size for sampling the image. This translates to 11.2 samples per μm or a maximum distance of 89 nm pixel width. To adjust to this criteria, a higher pixel number (1024×1024) and zoom factor (5.4×) was used. For Venus–Sec16AΔN, the calculated pixel size used was 43×43×130 (*x*, *y*, *z* in nm). Antibodies were sourced as follows: mouse monoclonal Sec31A and p150Glued (Transduction labs, BD Biosciences, Oxford, UK), giantin (Covance, Princeton, NJ), GalT (CellMab, Gothenburg, SE), α-tubulin (clone DM1A, Millipore, Watford, UK), Sec16A (Bethyl Labs, Montgomery, TX), rabbit polyclonal antibodies against Sec24C and Sec31A (Townley et al., 2008).

Live cell imaging

Cells grown on live cell dishes (MatTek, Ashland, MA) were imaged using a Perkin Elmer (Seer Green, UK) Ultraview ERS spinning disk confocal microscope with Photokinesis add-on running Volocity (version 5.3.2 build 0). The systems was attached to a Leica DMI6000 inverted microscope (Leica Microsystems, Milton Keynes, UK) with a Solent Scientific (Portsmouth, UK) incubator set to 37°C and a Leica HCX PL APO 63× 1.3 N.A. glycerol immersion lens mounted on a Piezo focus drive. Images were acquired with a Hamamatsu (Welwyn Garden City, UK) 9100-50 electron multiplying CCD. Cells were imaged in MEM without Phenol Red, supplemented with 30 mM HEPES, pH 7.4, 0.5 g l^{-1} sodium bicarbonate and 10% fetal calf serum. Venus-Sec16ΔN was imaged using a 514 nm laser with 405/440/514/640 nm band-pass filter and 587 nm emission filter. An exposure time of 400 mseconds and sensitivity of 165 was used. For mRuby–Sec23A a 568 nm laser was using with a 405/488/568/640 nm band-pass filter and 455/615 nm emission filter. Electron multiplier sensitivity was set to 165. The system was set to emission discrimination mode. For Fig. 1, 22×0.5 μm *z*-slices were acquired every minute for 90 time points (3 hours total imaging, 3330 images per time sequence). For Figs 3 and 4, 22×1 μm *z*-slices were acquired every 2 minutes for 90 time points (3 hours total imaging, 1980 images per time sequence). Shutters were managed for maximum sample protection.

For quantitative FRAP measurements a 63× 1.3 NA Plan-Apochromat objective was used. Photobleaching of Venus-Sec16AΔN was performed with a ~500 nm diameter circular region. Pre-bleach images were collected for 5 seconds and post-bleach images were collected for 60 seconds using 30% acousto-optical tunable filter power and low laser intensity. Background correction was performed by subtraction of a cytosolic region of interest within the cell periphery. ERES that moved out of focus or moved over 500 nm during the photobleaching series could not be analysed. Fluorescence recovery in the bleached region during the time series was quantified using Volocity 5 (Improvision) FRAP analysis software and exported for analysis to GraphPad Prism 4.02. Recycling kinetics were obtained by curve fitting to a one phase exponential $f(t)=A\bullet(1-e^{-kt})$ + B, Here, A is the mobile fraction, B is the fluorescence directly after photobleaching (%), and k is the rate of fluorescence recovery from which $t_{1/2}$ is determined [$t_{1/2}=\ln(2)/k$]. Statistical significance was determined using s.d. and the Student's unpaired *t*-test.

Quantification of image data

Image sequences were analysed using Volocity Quantitation to determine the number of puncta labelled with either Venus–Sec16AΔN or mRuby–Sec23A. Two methods were used, the first an automated count of all frames of multiple sequences (total 15 cells, >2000 individual puncta per time point from four different imaging experiments i.e. performed on different days). All slices in each image sequence were compressed to a single slice using maximum intensity. Cells were marked outlined using the region of interest (ROI) tool and all objects within that ROI of intensity between 9 and 100% with a size >0.1 μm but <5 μm (counted for each channel separately). For the graph shown in Fig. 3D these data were then averaged from 5 cells. It is important to note that this approach includes all objects conforming to these criteria. One can see clearly within such time sequences that many such objects do not in fact conform to our typical definition of an ERES in that brighter spots of mRuby–Sec23A labelling are frequently seen some distance from that of Venus–Sec16AΔN; this is not consistent with a bone fide functional ERES (Hughes et al., 2009). This automated approach, although unbiased, allows for inclusion of non-dividing cells impinging on the initially drawn region of interest during the time sequence. These factors combined lead to an overestimation of the number of defined puncta. Consequently, we also took a second approach applying slightly more stringent thresholding criteria (10–100% intensity, >0.1 μm, <0.5 μm) but manually drawing a region of interest around the dividing cell on a frame by frame basis. This was done for every tenth frame of two representative sequences (one of which is shown in Fig. 3A,B). This approach removed objects from outside the dividing cell and provides absolute quantification of bona fide ERES because of the requirement for increased intensity. This approach is in our opinion the more representative of the two because it does not detect transient accumulation of fluorescent signals that do not conform to our definition of an ERES.

Statistical analysis

Statistical differences between two groups of data were analysed with a two-tailed unpaired Student's *t*-test.

We are very grateful to Atsushi Miyawaki for Venus fluorescent protein, Mark Jepson and Alan Leard for assistance with confocal microscopy, Jon Lane, Pete Cullen, and members of the Stephens lab for helpful discussions and critical input to the manuscript. This work was funded by a Non-Clinical Senior Research Fellowship from the MRC (to D.J.S.) and a BBSRC PhD studentship (to H.H.). Deposited in PMC for release after 6 months.

Supplementary material available online at
http://jcs.biologists.org/cgi/content/full/123/23/4032/DC1

References

Altan-Bonnet, N., Sougrat, R., Liu, W., Snapp, E. L., Ward, T. and Lippincott-Schwartz, J. (2006). Golgi inheritance in mammalian cells is mediated through endoplasmic reticulum export activities. *Mol. Biol. Cell* **17**, 990-1005.

Bartz, R., Sun, L. P., Bisel, B., Wei, J. H. and Seemann, J. (2008). Spatial separation of Golgi and ER during mitosis protects SREBP from unregulated activation. *EMBO J.* **27**, 948-955.

Bhattacharyya, D. and Glick, B. S. (2007). Two mammalian Sec16 homologues have nonredundant functions in endoplasmic reticulum (ER) export and transitional ER organization. *Mol. Biol. Cell* **18**, 839-849.

Connerly, P. L., Esaki, M., Montegna, E. A., Strongin, D. E., Levi, S., Soderholm, J. and Glick, B. S. (2005). Sec16 is a determinant of transitional ER organization. *Curr. Biol.* **15**, 1439-1447.

Corthesy-Theulaz, I., Pauloin, A. and Pfeffer, S. R. (1992). Cytoplasmic dynein participates in the centrosomal localization of the Golgi complex. *J. Cell Biol.* **118**, 1333-1345.

Farmaki, T., Ponnambalam, S., Prescott, A. R., Clausen, H., Tang, B. L., Hong, W. and Lucocq, J. M. (1999). Forward and retrograde trafficking in mitotic animal cells.

ER-Golgi transport arrest restricts protein export from the ER into COPII-coated structures. *J. Cell Sci.* **112**, 589-600.

Hammond, A. T. and Glick, B. S. (2000). Dynamics of transitional endoplasmic reticulum sites in vertebrate cells. *Mol. Biol. Cell* **11**, 3013-3030.

He, C. Y., Pypaert, M. and Warren, G. (2005). Golgi duplication in Trypanosoma brucei requires Centrin2. *Science* **310**, 1196-1198.

Heinzer, S., Worz, S., Kalla, C., Rohr, K. and Weiss, M. (2008). A model for the self-organization of exit sites in the endoplasmic reticulum. *J. Cell Sci.* **121**, 55-64.

Henderson, M. C., Shaw, Y. J., Wang, H., Han, H., Hurley, L. H., Flynn, G., Dorr, R. T. and Von Hoff, D. D. (2009). UA62784, a novel inhibitor of centromere protein E kinesin-like protein. *Mol. Cancer Ther.* **8**, 36-44.

Ho, W. C., Allan, V. J., van Meer, G., Berger, E. G. and Kreis, T. E. (1989). Reclustering of scattered Golgi elements occurs along microtubules. *Eur. J. Cell Biol.* **48**, 250-263.

Hughes, H. and Stephens, D. J. (2008). Assembly, organization, and function of the COPII coat. *Histochem. Cell Biol.* **129**, 129-151.

Hughes, H., Budnik, A., Schmidt, K., Palmer, K. J., Mantell, J., Noakes, C., Johnson, A., Carter, D. A., Verkade, P., Watson, P. et al. (2009). Organisation of human ER-exit sites: requirements for the localisation of Sec16 to transitional ER. *J. Cell Sci.* **122**, 2924-2934.

Iinuma, T., Shiga, A., Nakamoto, K., O'Brien, M. B., Aridor, M., Arimitsu, N., Tagaya, M. and Tani, K. (2007). Mammalian Sec16/p250 plays a role in membrane traffic from the endoplasmic reticulum. *J. Biol. Chem.* **282**, 17632-17639.

Ivan, V., de Voer, G., Xanthakis, D., Spoorendonk, K. M., Kondylis, V. and Rabouille, C. (2008). Drosophila Sec16 mediates the biogenesis of tER sites upstream of Sar1 through an arginine-rich motif. *Mol. Biol. Cell* **19**, 4352-4365.

Kredel, S., Oswald, F., Nienhaus, K., Deuschle, K., Rocker, C., Wolff, M., Heilker, R., Nienhaus, G. U. and Wiedenmann, J. (2009). mRuby, a bright monomeric red fluorescent protein for labeling of subcellular structures. *PLoS ONE* **4**, e4391.

Kuge, O., Dascher, C., Orci, L., Rowe, T., Amherdt, M., Plutner, H., Ravazzola, M., Tanigawa, G., Rothman, J. E. and Balch, W. E. (1994). Sar1 promotes vesicle budding from the endoplasmic reticulum but not Golgi compartments. *J. Cell Biol.* **125**, 51-65.

Lucocq, J. M. and Warren, G. (1987). Fragmentation and partitioning of the Golgi apparatus during mitosis in HeLa cells. *EMBO J.* **6**, 3239-3246.

Mayer, T. U., Kapoor, T. M., Haggarty, S. J., King, R. W., Schreiber, S. L. and Mitchison, T. J. (1999). Small molecule inhibitor of mitotic spindle bipolarity identified in a phenotype-based screen. *Science* **286**, 971-974.

Nagai, T., Ibata, K., Park, E. S., Kubota, M., Mikoshiba, K. and Miyawaki, A. (2002). A variant of yellow fluorescent protein with fast and efficient maturation for cell-biological applications. *Nat. Biotechnol.* **20**, 87-90.

Palmer, K. J., Hughes, H. and Stephens, D. J. (2009). Specificity of cytoplasmic dynein subunits in discrete membrane-trafficking steps. *Mol. Biol. Cell* **20**, 2885-2899.

Prescott, A. R., Farmaki, T., Thomson, C., James, J., Paccaud, J. P., Tang, B. L., Hong, W., Quinn, M., Ponnambalam, S. and Lucocq, J. (2001). Evidence for prebudding arrest of ER export in animal cell mitosis and its role in generating Golgi partitioning intermediates. *Traffic* **2**, 321-335.

Seemann, J., Pypaert, M., Taguchi, T., Malsam, J. and Warren, G. (2002). Partitioning of the matrix fraction of the Golgi apparatus during mitosis in animal cells. *Science* **295**, 848-851.

Shima, D. T., Haldar, K., Pepperkok, R., Watson, R. and Warren, G. (1997). Partitioning of the Golgi apparatus during mitosis in living HeLa cells. *J. Cell Biol.* **137**, 1211-1228.

Souter, E., Pypaert, M. and Warren, G. (1993). The Golgi stack reassembles during telophase before arrival of proteins transported from the endoplasmic reticulum. *J. Cell Biol.* **122**, 533-540.

Steegmaier, M., Hoffmann, M., Baum, A., Lenart, P., Petronczki, M., Krssak, M., Gurtler, U., Garin-Chesa, P., Lieb, S., Quant, J. et al. (2007). BI 2536, a potent and selective inhibitor of polo-like kinase 1, inhibits tumor growth in vivo. *Curr. Biol.* **17**, 316-322.

Stephens, D. J. (2003). De novo formation, fusion and fission of mammalian COPII-coated endoplasmic reticulum exit sites. *EMBO rep.* **4**, 210-217.

Storrie, B., White, J., Rottger, S., Stelzer, E. H., Suganuma, T. and Nilsson, T. (1998). Recycling of golgi-resident glycosyltransferases through the ER reveals a novel pathway and provides an explanation for nocodazole-induced Golgi scattering. *J. Cell Biol.* **143**, 1505-1521.

Supek, F., Madden, D. T., Hamamoto, S., Orci, L. and Schekman, R. (2002). Sec16p potentiates the action of COPII proteins to bud transport vesicles. *J. Cell Biol.* **158**, 1029-1038.

Townley, A. K., Feng, Y., Schmidt, K., Carter, D. A., Porter, R., Verkade, P. and Stephens, D. J. (2008). Efficient coupling of Sec23-Sec24 to Sec13-Sec31 drives COPII-dependent collagen secretion and is essential for normal craniofacial development. *J. Cell Sci.* **121**, 3025-3034.

Ward, T. H., Polishchuk, R. S., Caplan, S., Hirschberg, K. and Lippincott-Schwartz, J. (2001). Maintenance of Golgi structure and function depends on the integrity of ER export. *J. Cell Biol.* **155**, 557-570.

Watson, P., Forster, R., Palmer, K. J., Pepperkok, R. and Stephens, D. J. (2005). Coupling of ER exit to microtubules through direct interaction of COPII with dynactin. *Nat. Cell Biol.* **7**, 48-55.

Watson, P., Townley, A. K., Koka, P., Palmer, K. J. and Stephens, D. J. (2006). Sec16 defines endoplasmic reticulum exit sites and is required for secretory cargo export in mammalian cells. *Traffic* **7**, 1678-1687.

Wei, J. H. and Seemann, J. (2009). Mitotic division of the mammalian Golgi apparatus. *Semin. Cell Dev. Biol.* **20**, 810-816.

Zaal, K. J., Smith, C. L., Polishchuk, R. S., Altan, N., Cole, N. B., Ellenberg, J., Hirschberg, K., Presley, J. F., Roberts, T. H., Siggia, E. et al. (1999). Golgi membranes are absorbed into and reemerge from the ER during mitosis. *Cell* **99**, 589-601.